

Article

# Cement Clinker Modified by Photocatalyst—Selected Mechanical Properties and Photocatalytic Activity during NO and BTEX Decomposition

Magdalena Janus <sup>1,\*</sup> , Jarosław Strzałkowski <sup>1</sup> , Kamila Zając <sup>1</sup> and Ewelina Kusiak-Nejman <sup>2</sup> 

<sup>1</sup> Faculty of Civil and Environmental Engineering, West Pomeranian University of Technology in Szczecin, al. Piastów 50, 70-311 Szczecin, Poland; jaroslaw.strzalkowski@zut.edu.pl (J.S.); kamila.zajac@zut.edu.pl (K.Z.)

<sup>2</sup> Faculty of Chemical Technology and Engineering, West Pomeranian University of Technology in Szczecin, ul. Pułaskiego 10, 70-310 Szczecin, Poland; ewelina.kusiak@zut.edu.pl

\* Correspondence: magdalena.janus@zut.edu.pl

**Abstract:** In this paper, a new way to obtain photoactive cements was presented. In this method amorphous TiO<sub>2</sub> is added to a cooler during the cooling of the cement clinker (Górażdże company) during cement production. Amorphous TiO<sub>2</sub> was taken from the installation for obtaining titanium dioxide using the sulphate method. During the study, amorphous TiO<sub>2</sub> was added to the clinker at 300, 600, 700, and 800 °C. The properties of the obtained cement were tested during the bending and compressive strength. The initial and the end of setting time was also measured. The adhesion of the obtained materials to concrete block, ceramic brick, and plasterboard were also evaluated. The photocatalytic activity of the obtained materials was studied during NO and BTEX (benzene, toluene, ethylbenzene, p-, m-, o-xylenes decomposition) decomposition. Cement with 5 wt% TiO<sub>2</sub> added to the clinker at 700 °C had the highest photocatalytic activity and the best mechanical properties.

**Keywords:** photocatalysis; photoactive cement; NO decomposition



**Citation:** Janus, M.; Strzałkowski, J.; Zając, K.; Kusiak-Nejman, E. Cement Clinker Modified by Photocatalyst—Selected Mechanical Properties and Photocatalytic Activity during NO and BTEX Decomposition. *Appl. Sci.* **2024**, *14*, 8855. <https://doi.org/10.3390/app14198855>

Academic Editor: Antonio Miotello

Received: 26 August 2024

Revised: 27 September 2024

Accepted: 30 September 2024

Published: 2 October 2024



**Copyright:** © 2024 by the authors. Licensee MDPI, Basel, Switzerland. This article is an open access article distributed under the terms and conditions of the Creative Commons Attribution (CC BY) license (<https://creativecommons.org/licenses/by/4.0/>).

## 1. Introduction

Photocatalysis is called reverse photosynthesis. During photosynthesis from carbon dioxide and water, organic compounds are produced. During photocatalysis, organic compounds are decomposed to carbon dioxide and water. This advanced oxidation process is used to modify the surface of building materials to give them self-cleaning and air purification properties. Plasters, glass panes, or photoactive paints are frequently used. Large surface structures, and the lack of need for additional painting after the use of photoactive materials, cause photocatalysis to arouse increased interest [1,2]. The current way to give photocatalytic activity to building materials is to coat their surface with special paints. Currently, however, photoactive cements, which could be used to obtain photoactive plasters without the need to cover them with additional layer paint, are gaining interest. Such photoactive cements can also be used for architectural cladding.

Photoactive cements are obtained by adding several types of photocatalysts to the finished cement, such as TiO<sub>2</sub> [3,4]. After adding nano-TiO<sub>2</sub> (NT) into cement-based composites, the induction period increased from 1.62 h to 2.83 h. The incorporation of TiO<sub>2</sub> reduces the Ca<sup>2+</sup> concentration in the solution and delays the nucleation of Ca(OH)<sub>2</sub> [3]. The hydration process of cement pastes mixed with NT particles consists of three processes: nucleation and crystal growth (NG), interaction at the phase boundary (I), and diffusion (D). These particles can promote cement hydration in NG process but reduce cement hydration rate in I and D processes. Another photocatalysts added to cement is SnO<sub>2</sub> [5]. Addition of these photocatalysts is responsible for the self-cleaning characteristic observed in these new building materials. Another material for cement modification is BiVO<sub>4</sub> [6]. Bismuth

vanadate ( $\text{BiVO}_4$ )-cement composites were coated on concrete surfaces. The photocatalytic activity of these composites was tested during the methylene blue (MB) dye degradation. These experiments showed that the 40 wt%  $\text{BiVO}_4$ -concrete pellets attained ~ 58% MB dye degradation efficiency. There are also cements with addition of  $\text{CeO}_2$  [7]. The addition of  $\text{CeO}_2$  nanoparticles promotes the creation of C–S–H gel which is the main hydration product which controls the mechanical properties of materials.

Presently cement is produced mainly by dry method. In the past wet method was also used. This dry method involves introducing cement flour into a kiln to produce clinker. The temperature used in the preparation of cement clinker is 1450–1500 °C. After leaving the furnace the hot clinker is passed through a cooler. The high difference between the temperature of the burning zone and beginning of cooling zone (about 1200 °C) is important for the best strength-giving properties [8]. In the cooler there is a temperature between 1200° and 100 °C. The time of residence of clinker in the cooler is about 30 min. In the case of obtaining photoactive cements, cooler seems to be the best place to introduce amorphous  $\text{TiO}_2$ . The aim of the study was to check at what temperature it is best to introduce amorphous  $\text{TiO}_2$  into the cooler and whether the time spent 30 min in the cooler is sufficient for the formation of a photoactive structure of  $\text{TiO}_2$ .

## 2. Materials and Methods

### 2.1. Modified Cements Preparation

An intermediate product from the titanium dioxide production plant by sulphate method (amorphous  $\text{TiO}_2$ ) was added to cement clinker (Górażdże company, Górażdże, Poland). Cement clinker was heated up to 300, 600, 700 and 800 °C. The amount of amorphous  $\text{TiO}_2$  was 1, 3 and 5 wt% of the clinker weight. After addition of amorphous  $\text{TiO}_2$  the 30 min cooling process took place. Modified cement clinker was ground together with 5 wt% gypsum obtained from the flue gas desulphurization installation of the Dolna Odra power plant (Dolna Odra, Poland) for 35 min at a speed of 450 rpm. During cooling amorphous materials transferred into crystalline structure. The results of XRD analysis and sulfur content of amorphous  $\text{TiO}_2$  annealed at different temperatures are presented in our earlier paper [9]. The sulfur content in the  $\text{TiO}_2$  samples calcined at different temperatures was 2% by weight. The average size of  $\text{TiO}_2$  crystallites was 7–8 nm. Designations of materials adopt in the studies in Table 1 were presented.

**Table 1.** Designations of materials adopted in the studies.

Designation	Abbreviation	The Temperature at Which the Clinker Was Heated [°C]	Weight % of $\text{TiO}_2$ to the Weight of Clinker	Weight % of Gypsum to the Weight of Clinker with $\text{TiO}_2$
clinker + 5% gypsum	clinker	-	-	5
clinker-300°C $\text{TiO}_2$ 1%	300/1	300	1	5
clinker300°C $\text{TiO}_2$ 3%	300/3	300	3	5
clinker300°C $\text{TiO}_2$ 5%	300/5	300	5	5
clinker600°C $\text{TiO}_2$ 1%	600/1	600	1	5
clinker600°C $\text{TiO}_2$ 3%	600/3	600	3	5
clinker600°C $\text{TiO}_2$ 5%	600/5	600	5	5
clinker700°C $\text{TiO}_2$ 5%	700/5	700	5	5
clinker800°C $\text{TiO}_2$ 1%	800/1	800	1	5
clinker800°C $\text{TiO}_2$ 3%	800/3	800	3	5
clinker800°C $\text{TiO}_2$ 5%	800/5	800	5	5

### 2.2. The Initial and Final of the Setting Time Measurements

Vicata Vicatronic automatic devices was used for measurements. The value of  $W/C = 0.30$  (water to cement) was applied to all variants of the tested grouts. Two measurements of the initial and final of the setting time were taken. The tests were conducted following the standard PN-EN 196-3:2016 [10]. The samples were stored under water at a temperature of  $20 \pm 1$  °C.

### 2.3. Determination of Bending and Compressive Strength of Standard Mortar

Testing machines (Walter + Bai, Löhningen, Switzerland) for strength measurements was used. The strength test was conducted based on the standard PN-EN 196-1:2016 [11]. A standard composition: 450 g of cement, 1350 g of standard sand and 225 g of water was used. The measurements were conducted at beams 4 cm × 4 cm × 16 cm. The value of  $W/C = 0.5$  was applied for all mortars. During first 24 h the samples were stored in a water bath with increased humidity. After 24 h, the samples were demolded and stored underwater until evaluated. The tests were performed after 28 days of curing. The bending strength measurements  $R_f$  were performed on three beams, and the measurements of compressive strength  $R_c$  were performed on six specimens.

### 2.4. Adhesive Strength

The tests for the adhesive strength of cement mortars to the substrate were conducted in accordance with the requirements of the PN-EN 1015-12:2016 standard [12]. The tests covered ceramic, concrete and plasterboard surfaces. The surfaces of the substrate materials were mechanically dedusted and primed with an appropriate primer for the given material, and then moistened with water. For the tested cements, the standard mortar composition was used: 450 g of cement, 1350 g of standard silica sand and 225 g of water. A 10 mm layer of mortar was applied to the surface of individual materials, using side profiles to maintain the same thickness over the entire surface of the element. For each type of mortar, a minimum of four discs were prepared for a given type of substrate. The specimens were stored for 28 days in a climatic chamber with a temperature of  $20 \pm 1$  °C and RH > 95%. The day before the test, metal discs were glued to specific places on the surface using a two-component epoxy adhesive. The tests were performed after 28 days of the mortar curing on the surface of the substrate materials. The pull off device (Baustoff-Prüfssysteme Wennigsen GmbH; model F20D Easy M2000, Köln, Germany) was used to break the mortar from the substrate.

### 2.5. Photocatalytic Activity Test

The photocatalytic activity of prepared cement plates towards the degradation of air pollution was also proved. The NO gas (1.989 ppm ± 0.040 ppm, Air Liquide, Kraków, Poland) was used as model pollution. NO<sub>x</sub> removal was evaluated using the experimental installation, which scheme is presented in Figure 1.

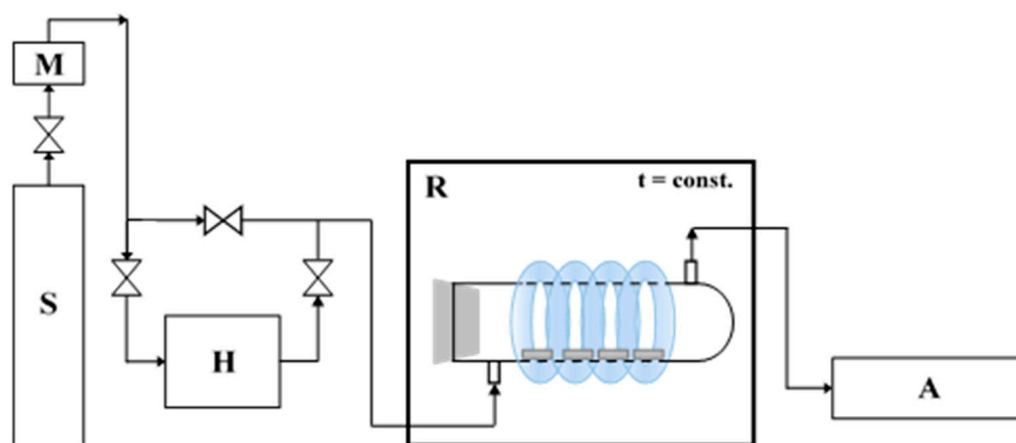


**Figure 1.** The scheme of the system to photocatalytic removal of NO (S—a source of pollution; M—mass flow; H—humidifier; R—photocatalytic reactor with irradiation source; A—NO<sub>x</sub> analyzer [9]).

Eight studied cement plates (one at dimensions of 2 cm × 2 cm × 0.5 cm) were placed in the central part of the cylindrical reactor (pyrex glass; Ø × H = 9 cm × 32 cm). Used NO was diluted with humidified synthetic air (50% humidity) to obtain 1 ppm and 0.2 ppm

initial concentration, the flow rate through reactor was  $500 \text{ cm}^3/\text{min}$ , gas temperature was  $25 \text{ }^\circ\text{C}$ . The equilibrium of dark conditions reach after 35 min, then UV lamps were turned on for 30 min. The irradiation cumulative intensity of  $100 \text{ W/m}^2$  UV and  $4 \text{ W/m}^2$  Vis was used for measurements. T200 NO<sub>x</sub> analyzer (Teledyne, San Diego, CA, USA) was used for NO and NO<sub>2</sub> measurements.

In Figure 2 the scheme of installation for photocatalytic removal of BTEX is presented. Two studied cement plates (one at dimensions of  $8 \text{ cm} \times 4 \text{ cm} \times 1 \text{ cm}$ ) were placed inside the reactor (Heraeus type reactor UV-RS-2;  $\text{Ø} \times \text{H} = 8 \text{ cm} \times 21 \text{ cm}$ ) with a medium pressure mercury vapor lamp (TQ-150,  $\lambda_{\text{max}} = 365 \text{ nm}$ ,  $I = 146 \text{ W/m}^2$ ). The irradiation time during photocatalysis process was 10 min. The BTEX mixture (benzene 5 ppm, ethyl benzene 5 ppm, toluene 5 ppm, o-, p-, m-xylene 5 ppm) (AG Gases & Equipment, Stoke-on-Trent, UK) was diluted with humidified synthetic air (50% humidity) in a ratio 1:1. The oxygen and water molecules were necessary for forming oxidative species, which are essential in photocatalytic reactions. The polluted air flowed through the reactor for 10 min at a rate of  $500 \text{ cm}^3/\text{min}$ . After 10 min outlet and flow were stop. Smart SPME Arrow (phase type: Divinylbenzene (DVB)/Polydimethylsiloxane (PDMS), phase thickness  $120 \text{ }\mu\text{m}$ ) were used for gases analysis. Smart SPME Arrow was introduced into the reactor for 2 min and after that to injector into the GC–MS apparatus (Nexis GC-2030, Shimadzu, Japan), which consisted of a single quadrupole mass spectrometer model QP2020 NX ISQ, (Shimadzu, Japan). A capillary column Zebron-PAH (30 m length,  $0.25 \text{ mm}$  I.D. The starting oven temperature was held at  $45 \text{ }^\circ\text{C}$  for 2 min and ramped to  $105 \text{ }^\circ\text{C}$  at a rate of  $10 \text{ }^\circ\text{C}/\text{min}$ .

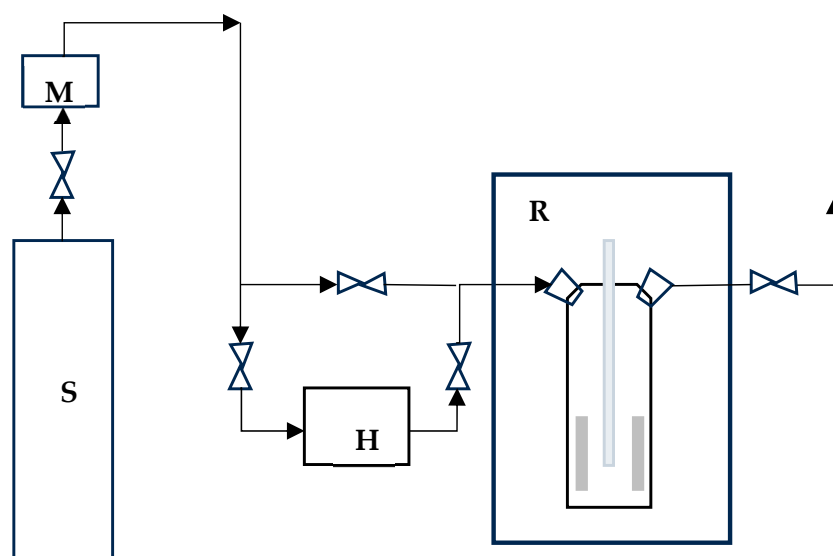


**Figure 2.** The scheme of installation for photocatalytic removal of BTEX (S—a source of pollution; M—mass flow; H—humidifier; R—photocatalytic reactor with irradiation source).

### 3. Results and Discussion

#### 3.1. Mechanical Properties of Obtained Modified Clinker

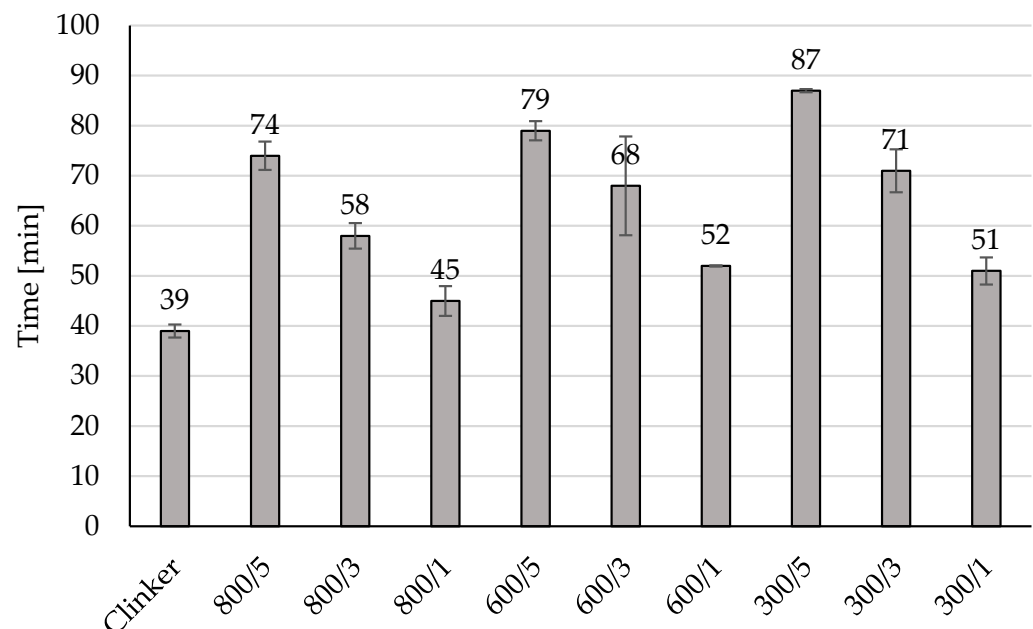
In Table 2 the bending strength and compressive strength values of modified clinker ground with gypsum are presented. The bending strength slightly increased with increasing of TiO<sub>2</sub> presence but close to unmodified material. The highest increasing of this value was 22% for materials 700/5. The compressive strength at 28 days of curing increased slightly with the TiO<sub>2</sub> content, with this being especially notable in the sample with 5wt% of TiO<sub>2</sub>. The highest value of compressive strength in the case of two modified clinker 600/1 and 600/3 addition of amorphous TiO<sub>2</sub> decrease the bending strength about 2% and 8%, respectively. In other cases, the addition of amorphous TiO<sub>2</sub> to the clinker during its cooling increased the bending strength from a slight 1% for material 800/1 to 25% for clinker 300/5.

**Table 2.** The values of bending and compressive strength for modified clinkers.

Materials	The Bending Strength [MPa]	Standard Deviation	The Compressive Strength [MPa]	Standard Deviation
clinker	5.24	0.11	35.27	0.88
300/1	5.57	0.02	36.20	1.67
300/3	5.38	0.04	34.17	1.44
300/5	6.56	0.50	42.67	1.66
600/1	5.12	0.39	35.17	0.63
600/3	4.83	0.30	30.57	1.73
600/5	5.95	0.29	41.04	0.82
700/5	6.41	0.19	41.53	2.37
800/1	5.37	0.14	33.95	1.83
800/3	5.30	0.22	35.32	0.78
800/5	5.63	0.21	38.56	2.03

### 3.2. The Initial and Final of the Setting Time Measurements

Addition of amorphous  $\text{TiO}_2$  during clinker cooling may be a good way for controlling the initial and final of the setting time as it can be observed in Figure 3, 5 wt% addition of amorphous  $\text{TiO}_2$  increased the initial of setting time from 39 min for unmodified material to 87 min for material 300/5, to 79 min for material 600/5 and to 74 min for 800/5. In all prepared materials modification increased the initial of setting time from 6 min (for 800/1) to 39 min (for 300/5). The same observed can be done for the values of the final of the setting time presented in Figure 4, 5 wt% of amorphous  $\text{TiO}_2$  has the highest influence on increasing of this value of the final of the setting time, from 89 min for unmodified material to 135 min for 300/5, to 126 min for 600/5 and to 127 min for 800/5. Adding a semi-finished product from the titanium dioxide installation using the sulphate method to the clinker during its cooling resulted in the clinker being surrounded by a layer of  $\text{TiO}_2$ . During grinding,  $\text{TiO}_2$  was in very good contact with the clinker and did not form agglomerates, which influenced the increase in the time of the initial and end of setting time.

**Figure 3.** The initial setting time of the modified clinkers.

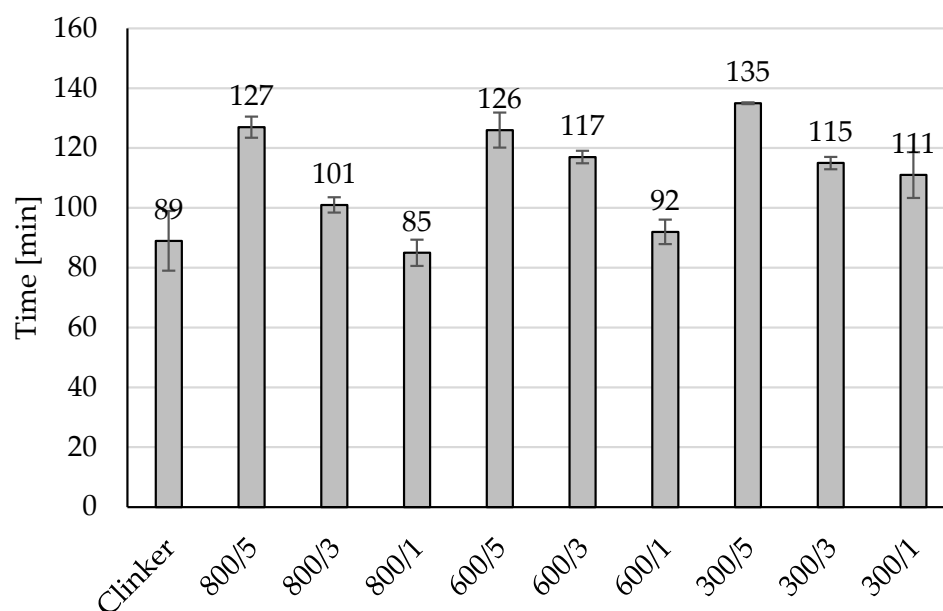


**Figure 4.** The final setting time of the modified clinkers.

### 3.3. Photocatalytic Activity Tests

#### 3.3.1. NO Decomposition

The photocatalytic activity of the new photoactive cements was evaluated during the decomposition of NO(II) under UV radiation, the results are presented in Table 3. During the tests, no influence of clinker temperature on the degree of NO decomposition was observed. In the case where the research was conducted at lower concentrations of NO, it follows that at 5 wt% of the TiO<sub>2</sub> content the highest NO decomposition is achieved. The highest photocatalytic activity was achieved by the 700/5 material. During 30 min of UV exposure to eight plates of modified clinker in NO streams with a concentration of 0.2 ppm, the NO removal rate was 14.4%.

**Table 3.** Photocatalytic decomposition of NO with an initial concentration of 1 and 0.2 ppm under UV light irradiation.

Materials	NO Decomposition [%]	
	1 ppm	0.2 ppm
Clinker	2.0	2.7
300/1	3.7	5.9
300/3	5.2	7.0
300/5	3.0	7.8
600/1	5.0	6.0
600/3	7.4	7.8
600/5	8.3	9.5
700/5	6.0	14.4
800/1	4.8	7.6
800/3	5.5	5.0
800/5	5.1	10.9

#### 3.3.2. BTEX Decomposition

The photocatalytic activity was evaluated during BTEX decomposition. The mixture of benzene, toluene, ethyl benzene and xylenes were used. The obtained results in Figure 5 were presented. Initially, the gas mixture was passed through the reactor for 10 min to achieve the complete filling of the reactor space with the gas. After 10 min, the outlet and inlet of the gases was closed. A Smart SPME Arrow was introduced into the gas reactor and for 2 min the gases were sorbed on the bed. After 2 min, the Smart SPME Arrow was

inserted into the chromatograph injector and subjected to 1 min of desorption. The mass detector was used to measure gases concentration, obtained values were marked as the initial concentration, marked on the graph as 100%. Then, two plates made of unmodified clinker were placed in the reactor and the procedure of filling the reactor with gases and the procedure of determining the concentration with Smart SPME Arrow were repeated. As can be seen in Figure 5, ethyl benzene and xylenes have been adsorbed on the surface of the unmodified clinker in the amount of 7% and 13%, respectively. After adsorption studies, studies on photolysis in the presence of unmodified clinker and photocatalysis in the presence of modified clinker were started. After 10 min of UV light irradiation, as it can be seen in Figure 5, there was a partial desorption of gases from the clinker surface, which is particularly visible in the case of ethyl benzene, whose concentration increased by 4%. In addition, it can be noted that after switching on UV radiation, partial photolysis of gases (ethyl benzene and xylenes were decomposed) occurred, as there was a clear increase in the concentration of benzene (by 21%) and toluene by (27%). Since research on the breakdown of BTEX is expensive, only one material has been selected for these tests, which has the highest applicability. It is a material that was created because of the addition of 5wt% amorphous  $\text{TiO}_2$  to cement clinker at a temperature of 700 °C. As can be seen in Figure 5, after 10 min of irradiation, the level of ethyl benzene (by 37%) and xylene (by 62%) was significantly reduced. There was an increase in benzene concentration (by 25%), the level of toluene remained unchanged. These results mean that in the process of photocatalysis, the ethyl group of ethyl benzene and methyl group of xylenes broke off, which resulted in an increase in the concentration of benzene. The increase in benzene concentration is not proportional to the decrease in ethylbenzene and xylenes concentrations. Benzene can be oxidized, the formation of phenol, benzoquinone, and hydroquinone certainly also occurred. When the benzene ring is decomposed the formation of such products as  $\text{CO}_2$  and CO occurs [13,14].

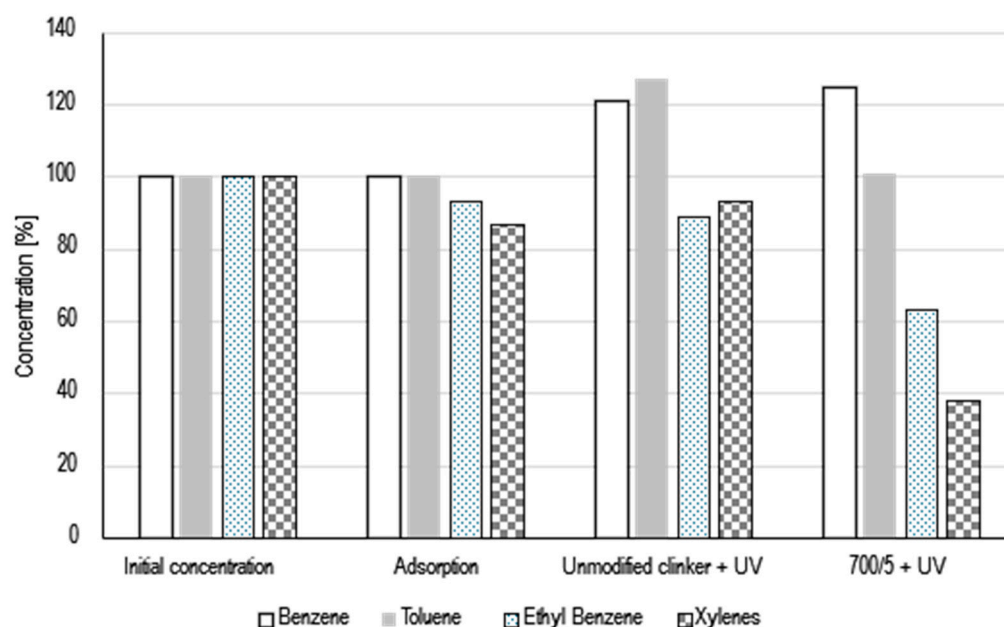


Figure 5. Photocatalytic decomposition of BTEX with under UV light irradiation.

### 3.4. Adhesive Strength

The best photocatalytic activity during NO decomposition and acceptable values of compressive and bending strength has material 700/5. For this material, the adhesive strength tests were done. Three different substrates, such as ceramic, concrete, plasterboard, the most used in construction, were selected to perform the adhesion tests. As can be seen in Table 4, the modification of  $\text{TiO}_2$  clinker resulted in an improvement in the adhesion of

these modified materials to all tested surfaces. The increase in adhesion was highest in the case of concrete, as the addition of TiO<sub>2</sub> improved adhesion by as much as 39%, and the lowest in the case of ceramics, as the addition of TiO<sub>2</sub> improved adhesion by 21%. Material 700/5 has almost the highest values of bending and compressive strength and elongate initial and final setting time. This longer time before the setting process begins can cause the material to penetrate the substrate better, resulting in a stronger connection between the materials and therefore increased adhesion.

**Table 4.** The values of adhesive strength for modified clinkers.

Materials	Adhesive Strength [MPa]					
	Ceramic	Standard Deviation	Concrete	Standard Deviation	Plasterboard	Standard Deviation
clinker	1.598	0.333	0.787	0.200	0.486	0.071
700/5	1.932	0.323	1.287	0.176	0.630	0.044

#### 4. Conclusions

The research has shown that the new method of obtaining photoactive cements can be used when clinkers from various manufacturers are used. In our previous research, we used Lafarge film clinker [9], the research presented in the article was conducted with the use of Górażdże clinker. In addition, we can see that the obtained photoactive cement can be used to remove volatile organic compounds from the air. After 10 min of irradiation, the level of ethyl benzene decreased by 37% and xylene decreased by 62%. In addition, the modification leads to a material that is characterized by higher adhesion to ceramics, concrete and plasterboard. Adhesion to concrete increased by 39%, adhesion to ceramics increased by 21% and adhesion to plasterboard increased by 30%. The studies showed that the best materials from mechanical and photocatalytic activity view is possible to obtained by addition of an intermediate product from the titanium dioxide production plant by sulphate method (amorphous TiO<sub>2</sub> 5 wt%) to clinker at 700 °C.

**Author Contributions:** Conceptualization, M.J.; methodology, M.J., J.S. and E.K.-N.; formal analysis, M.J., J.S. and E.K.-N.; investigation, M.J., J.S., K.Z. and E.K.-N.; writing—original draft preparation, M.J.; writing—review and editing, M.J.; visualization, M.J.; supervision, M.J.; project administration, M.J.; funding acquisition, M.J. All authors have read and agreed to the published version of the manuscript.

**Funding:** This research was funded by National Centre for Research and Development program Tango V (TANGO-V-A/0012/2021-00).

**Institutional Review Board Statement:** Not applicable.

**Informed Consent Statement:** Not applicable.

**Data Availability Statement:** The original contributions presented in the study are included in the article, further inquiries can be directed to the corresponding author.

**Conflicts of Interest:** The authors declare no conflicts of interest.

#### References

- Janus, M.; Mađraszewski, S.; Zajac, K.; Kusiak-Nejman, E. A new preparation method of cement with photocatalytic activity. *Materials* **2020**, *13*, 5540. [[CrossRef](#)] [[PubMed](#)]
- Bianchi, C.L.; Cerrato, G.; Pirola, C.; Galli, F.; Capucci, V. Photocatalytic porcelain grés large slabs digitally coated with AgNPs-TiO<sub>2</sub>. *Environ. Sci. Pollut. Res.* **2019**, *26*, 36117–36123. [[CrossRef](#)] [[PubMed](#)]
- Liu, Y.; Guo, H.; Zhang, Z.; Zhu, Y. Hydration mechanism and photocatalytic antibacterial performance of cement-based composites modified by hydrophilic nano-TiO<sub>2</sub> particles. *Constr. Build. Mater.* **2024**, *419*, 135538. [[CrossRef](#)]
- Kuang, Y.; Ding, F.; Peng, Z.; Fan, F.; Zhang, Z.; Ji, X. Photocatalytic Degradation of Vehicle Exhaust by Nano-TiO<sub>2</sub> Cement Slurry: Experimental Factors and Field Application. *Catalysts* **2024**, *14*, 21. [[CrossRef](#)]
- Vendramini, D.; Benatto, V.G.; Ashtiani, A.M.; La Porta, F. Photocatalytic Applications of SnO<sub>2</sub> and Ag<sub>2</sub>O-Decorated SnO<sub>2</sub> Coatings on Cement Paste. *Catalysts* **2023**, *13*, 1479. [[CrossRef](#)]



6. Kumar, M.; Elqahtani, Z.M.; Alrowaili, Z.A.; Al-Buriah, M.S.; Kebaili, I.; Boukhris, I.; Vaish, R. Photocatalytic BiVO<sub>4</sub>-Cement Composites for Dye Degradation. *J. Electr. Mater.* **2023**, *52*, 4672–4685. [[CrossRef](#)]
7. Ibrahim, S.M.; Heikal, M.; Mohamed, O.A. Performance of CeO<sub>2</sub>-nanoparticles on the mechanical and photocatalytic properties of composite cement. *J. Build. Eng.* **2023**, *68*, 106162. [[CrossRef](#)]
8. Hewlett, P. (Ed.) *Lea's Chemistry of Cement and Concrete*; Elsevier Science & Technology: Amsterdam, The Netherlands, 2003.
9. Janus, M.; Strzałkowski, J.; Zając, K.; Kusiak-Nejman, E. New Method for Photoactive Cement Preparation Selected Mechanical Properties and Photocatalytic Activity of New Materials. *Materials* **2023**, *17*, 2285. [[CrossRef](#)] [[PubMed](#)]
10. *Standard PN-EN 196-3:2016; Cement Test Methods—Part 3: Determination of Setting Times and Volume Constancy*. Polish Committee for Standardization: Warsaw, Poland, 2016.
11. *Standard PN-EN 196-1:2016; Cement Test Methods—Part 1: Determination of Strength*. Polish Committee for Standardization: Warsaw, Poland, 2016.
12. *PN-EN 1015-12:2016; Test Methods for Mortars—Part 12: Determination of Adhesion to the Substrate of Hardened Mortars for Exterior and Interior Plastering*. Polish Committee for Standardization: Warsaw, Poland, 2016.
13. d'Hennezel, O.; Pichat, P.; Ollis, D.F. Benzene and toluene gas-phase photocatalytic degradation over H<sub>2</sub>O and HCl pretreated TiO<sub>2</sub>: By-products and mechanisms. *J. Photochem. Photobiol. A Chem.* **1998**, *118*, 197–204. [[CrossRef](#)]
14. Zhang, S.; Zheng, Z.; Wang, J.; Chen, J. Heterogeneous photocatalytic decomposition of benzene on lanthanum-doped TiO<sub>2</sub> film at ambient temperature. *Chemosphere* **2006**, *65*, 2282–2288. [[CrossRef](#)] [[PubMed](#)]

**Disclaimer/Publisher's Note:** The statements, opinions and data contained in all publications are solely those of the individual author(s) and contributor(s) and not of MDPI and/or the editor(s). MDPI and/or the editor(s) disclaim responsibility for any injury to people or property resulting from any ideas, methods, instructions or products referred to in the content.